Neutrino oscillations in dense neutrino gases

Stuart Samuel*
Department of Physics, Indiana University, Bloomington, Indiana 47405
and Department of Physics, The City College of New York, New York, New York 10031†
(Received 8 February 1993)

We consider oscillations of neutrinos under conditions in which the neutrino density is sufficiently large that neutrino-neutrino interactions cannot be neglected. A formalism is developed to treat this highly nonlinear system. Numerical analysis reveals a rich array of phenomena. In certain gases, a self-induced Mikheyev-Smirnov-Wolfenstein effect occurs in which electron neutrinos are resonantly converted into muon neutrinos. In another relatively low-density gas, an unexpected parametric resonant conversion takes place. Finally, neutrino-neutrino interactions maintain coherence in one system for which *a priori* one expected decoherence.

PACS number(s): 95.30.Cq, 13.15.−f, 14.60.Gh

I. INTRODUCTION

In the 1990s progress in astrophysics has accelerated, largely due to the use of satellite-based experiments. More and more is being discovered about how the Universe has evolved since the big bang, about the global distribution of galaxies and matter, and about the nature of exotic astrophysical objects such as pulsars, neutron stars, and black holes. Neutrinos are potentially a useful source of information. Like photons that were left behind as an early-Universe relic (the cosmic microwave background radiation), neutrinos should also obey a thermal distribution governed by a temperature $(\frac{4}{11})^{1/3}$ times the photon temperature [1]. Since neutrinos decoupled earlier than photons, the detection of the cosmic neutrino relic would provide a glimpse of our Universe at a very early stage. They are excellent probes of astrophysical objects since they often escape without interaction because of their very weak coupling to matter. An example is for the Sun, where Earth-based neutrino detectors allow the exploration of the physics of the Sun's core. Another example is SN 1987A for which neutrinos provided useful information.

If neutrinos have masses and mixing angles then the physics becomes even more interesting because of neutrino oscillations. Such oscillations can have a dramatic effect on the use of neutrinos as experimental probes. A prominent example is for solar neutrinos. For certain values of neutrino masses and mixing angles, the electrons in the Sun cause resonant conversion. Electron neutrinos produced in the core can emerge from the Sun's surface as muon neutrinos. The Mikheyev-Smirnov-Wolfenstein (MSW) effect [2,3] is a popular explanation of the solar neutrino problem [4].

Although no definite evidence exists for nonzero neutrino masses (there are only experimental upper limits), many theoretical frameworks predict masses too small to have been detected [5]. Left-right-symmetric models, as well as SO(10), E_6 and many other grand-unified theories, contain right-handed neutrinos [6]. In these theories and many extensions of the standard model, neutrinos have masses and mix. Neutrinos frequently have masses in string theories.

In the early stages of cosmological history, neutrinos constituted a dense gas. In this and other astrophysical settings the interactions of neutrinos with themselves cannot be neglected. In this paper we investigate the physics of a dense neutrino gas under the assumption that neutrinos have masses and mix. The system is not so easy to analyze for the following reason. The oscillation of a particular neutrino is affected by the electron neutrinos and muon neutrinos through which it travels. If the background neutrino density is known, it is straightforward to compute the effect on the oscillation of a single neutrino. However, all the neutrinos in the gas are oscillating and it is not easy to ascertain the flavor content of the background. This system has appeared in the context of other computations [7–13]. As pointed out in Refs. [13,14], there are subtleties concerning dense neutrino gases. Often incorrect assumptions have been used. Reference [14] determined the correct equations for a system consisting of two neutrinos, but the case of a multiparticle gas was unsolved.

One of our main results is a formalism to handle neutrino oscillations for a dense neutrino gas. In Sec. II we derive the equations governing a general system. The propagation of a single neutrino is determined under the assumption that the background neutrino currents are known. Knowledge of many such individual solutions should suffice in determining the background. Indeed, based on an approach similar to the Hartree-Fock approximation, we derive self-consistency equations for the backgrounds.

We hope to apply our methods to early-Universe physics, supernova explosions, and neutron stars. Since the concept of a neutrino gas is general, there may be unforeseen applications.

In addition to the average density, neutrino masses,

*Electronic address: SAMUEL@SCI.CCNY.CUNY.EDU
†Permanent address.

and neutrino mixing angles, the determination of the backgrounds depends on statistical features of the gas, such as the energy distribution of neutrinos, fluctuations in the density of backgrounds, and the initial distribution of neutrinos in flavor space. Hence, the physics depends on certain features of the gas. This renders it difficult to make general statements about oscillations for a dense neutrino gas. The subtleties here are sufficiently important that part of Sec. II is devoted to them.

In Sec. III we treat the homogeneous gas. Translational symmetry significantly simplifies the analysis. In addition, there is a formulation of the problem which resembles a particle moving in a magnetic field and permits one to use physical intuition. We also derive in Sec. III the analogue of the adiabatic approximation. One general result is that, at late times, the backgrounds tend to become diagonal in the mass-eigenstate basis and not in the flavor basis, as one might assume. In Sec. IV we present exploratory numerical analyses. The examples considered use idealized statistical distributions but are sufficient for exhibiting possible behaviors of physical gases. We restrict ourselves to the two-flavor case for reasons of simplicity and call the two flavors electron and muon.

A neutrino gas is a highly nonlinear system in which unexpected phenomenon may occur. We have observed four generic types of behavior.

(1) The neutrinos oscillate more or less as they would in a vacuum. Such a behavior often occurs, as expected, when the gas is not too dense. The effect of background neutrinos is minimal.

(2) There is a self-induced MSW effect. A gas initially consisting of electron neutrinos turns into a gas consisting mostly of muon neutrinos within a few oscillation times. The matter-induced mixing angle evolves from a value around $\pi/2$ to a value near zero. There is resonant conversion of electron neutrinos into muon neutrinos. This behavior seems to happen only when the gas is dense and neutrino self-interaction effects are maximal.

(3) For one type of gas in which the neutrino density was relatively small, a parametric resonance occurred. During many oscillation times the electron neutrinos slowly converted into a gas of mostly muon neutrinos. The background oscillated with a small amplitude but in phase with individual neutrinos, so that during each oscillation period a small fraction of electron neutrinos was converted into muon neutrinos on average. Maximal conversion occurred and the effects of neutrino interactions were dramatically enhanced on large time scales.

(4) For another type of gas, self-maintained coherence occurred. One expects statistical distributions to cause individual neutrinos to have different oscillation times and to not be in phase. Thus, for sufficiently large times, cancellations should occur to produce a smooth average background neutrino density. The backgrounds should achieve constant asymptotic values. Instead, we found that neutrino-neutrino interactions caused the oscillations to remain in phase and decoherence did not occur. This phenomenon took place for a relatively dense system and arose due to the nonlinear nature of the problem.

Behaviors (3) and (4) were unexpected. Behavior (1) is quite reasonable. Behavior (2) can be understood somewhat intuitively. Roughly speaking, it is similar to the MSW effect with background electron neutrinos replacing the Sun's electrons and with time playing the role of radial distance. A significant difference is the presence of off-diagonal backgrounds (see Sec. II). As in the MSW effect, the matter-induced mixing angle starts near 90° for a sufficiently dense gas. The initial electron neutrinos begin to oscillate, so that, after a short time, the background electron neutrino density is reduced. The situation is similar to a neutrino moving a little outward from the Sun's core; the electron density goes from a high value to a smaller value. In the next time interval, the neutrinos oscillate in a less dense background causing a little more conversion. The background is further reduced and so on. The only question is whether the process slows down and stops before passing through the resonance. If it continues, the final mixing angle is small and a large fraction of the initial electron neutrinos are converted to muon neutrinos. In this case, the final situation is like that of a neutrino emerging from the Sun's surface.

We work in units for which $\hbar = c = 1$. Although our formalism gives basis-independent results, we generally work in the flavor eigenstate basis for which Z^0 and $W^{\pm}$ couple to currents with no off-diagonal terms.

II. THE NEUTRINO GAS: GENERAL CONSIDERATIONS AND FORMALISM

A. The background interactions

The propagation of a neutrino through a medium is affected by the presence of other leptons. A well-known example occurs for the Sun. For certain ranges of neutrino masses and mixing angles, the interaction of neutrinos with the Sun's electrons greatly affects neutrino oscillations and leads to resonant conversion. This is the well-known MSW effect [2,3].

Interactions which are the same for all flavors of neutrinos do not affect neutrino oscillations. An example is the neutral-current interaction due to electrons via the exchange of Z^0. In contrast, electrons interact only with electron neutrinos in the charge-current interaction produced by the exchange of $W^{\pm}$. The corresponding four-fermion Lagrangian $\mathcal{L}_{\rm int}^{\rm CC}$ is

$$\mathcal{L}_{\rm int}^{\rm CC} = -2\sqrt{2}G_F[\bar{e}_L\gamma^\lambda\nu_{eL}(\mathbf{x},t)\bar{\nu}_{eL}\gamma_\lambda e_L(\mathbf{x},t) + \bar{\mu}_L\gamma^\lambda\nu_{\mu L}(\mathbf{x},t)\bar{\nu}_{\mu L}\gamma_\lambda\mu_L(\mathbf{x},t)] , \quad (2.1)$$

where G_F is Fermi's constant, and e, μ, ν_e, and ν_μ are, respectively, the fields for the electron, muon, electron neutrino, and muon neutrino. The subscript L means a left-handed fermion:

$$\psi_L = [(1-\gamma_5)/2]\psi .$$

To save space, we do not always display the $\mathbf{x}$ and t dependence.

By a Fierz transformation Eq. (2.1) can be rewritten as

$$\mathcal{L}_{\rm int}^{\rm CC}=-2\sqrt{2}G_F(\bar{e}_L\gamma^\lambda e_L\bar{\nu}_{eL}\gamma_\lambda\nu_{eL}+\bar{\mu}_L\gamma^\lambda\mu_L\bar{\nu}_{\mu L}\gamma_\lambda\nu_{\mu L})\ . \tag{2.2}$$

In the classical limit, the left-handed current $\bar{e}_L\gamma^\lambda e_L(\mathbf{x},t)$ is replaced by its background value $\langle\bar{e}_L\gamma^\lambda e_L(\mathbf{x},t)\rangle$. The same is true for the left-handed muon current. Consequently,

$$\begin{aligned}\mathcal{L}_{\rm int}^{\rm CC}\rightarrow&-\frac{G_F}{\sqrt{2}}(2\langle\bar{e}_L\gamma^\lambda e_L\rangle-2\langle\bar{\mu}_L\gamma^\lambda\mu_L\rangle)(\bar{\nu}_{eL}\gamma_\lambda\nu_{eL}-\bar{\nu}_{\mu L}\gamma_\lambda\nu_{\mu L})\\&-\frac{G_F}{\sqrt{2}}(2\langle\bar{e}_L\gamma^\lambda e_L\rangle+2\langle\bar{\mu}_L\gamma^\lambda\mu_L\rangle)(\bar{\nu}_{eL}\gamma_\lambda\nu_{eL}+\bar{\nu}_{\mu L}\gamma_\lambda\nu_{\mu L})\ .\end{aligned} \tag{2.3}$$

Only the first term treats electron neutrinos and muon neutrinos differently, and hence is relevant for oscillations.

When the neutrino currents are as large as charged-lepton currents, the interaction of neutrinos with themselves must be included. The exchange of a Z^0 leads to the four-fermion interactions

$$\begin{aligned}\mathcal{L}_{\rm int}^{\rm NC}=-\frac{G_F}{\sqrt{2}}&(\bar{\nu}_{eL}\gamma^\lambda\nu_{eL}\bar{\nu}_{eL}\gamma_\lambda\nu_{eL}+\bar{\nu}_{\mu L}\gamma^\lambda\nu_{\mu L}\bar{\nu}_{\mu L}\gamma_\lambda\nu_{\mu L}\\&+2\bar{\nu}_{eL}\gamma_\lambda\nu_{eL}\bar{\nu}_{\mu L}\gamma^\lambda\nu_{\mu L})\ .\end{aligned} \tag{2.4}$$

Let us mimic the procedure for the charged-current case. We replace left-handed neutrino currents by background values using

$$\begin{aligned}\mathcal{L}_{\rm int}^{\rm NC}\rightarrow&-\frac{3G_F}{\sqrt{2}}[(\langle\bar{\nu}_{eL}\gamma^\lambda\nu_{eL}\rangle+\langle\bar{\nu}_{\mu L}\gamma^\lambda\nu_{\mu L}\rangle)(\bar{\nu}_{eL}\gamma_\lambda\nu_{eL}+\bar{\nu}_{\mu L}\gamma_\lambda\nu_{\mu L})]\\&-\frac{G_F}{\sqrt{2}}[(\langle\bar{\nu}_{eL}\gamma^\lambda\nu_{eL}\rangle-\langle\bar{\nu}_{\mu L}\gamma^\lambda\nu_{\mu L}\rangle)(\bar{\nu}_{eL}\gamma_\lambda\nu_{eL}-\bar{\nu}_{\mu L}\gamma_\lambda\nu_{\mu L})]\\&-\frac{G_F}{\sqrt{2}}(2\langle\bar{\nu}_{eL}\gamma^\lambda\nu_{\mu L}\rangle\bar{\nu}_{\mu L}\gamma_\lambda\nu_{eL}+2\langle\bar{\nu}_{\mu L}\gamma^\lambda\nu_{eL}\rangle\bar{\nu}_{eL}\gamma_\lambda\nu_{\mu L})+\text{const}\ .\end{aligned} \tag{2.5}$$

There are two subtleties involved in deriving Eq. (2.5). The first is that each four-fermion interaction produces several terms when one uses

$$\begin{aligned}\bar{\psi}_{aL}\gamma^\lambda\psi_{bL}\bar{\psi}_{cL}\gamma_\lambda\psi_{dL}\rightarrow&\bar{\psi}_{aL}\gamma^\lambda\psi_{bL}\langle\bar{\psi}_{cL}\gamma_\lambda\psi_{dL}\rangle+\langle\bar{\psi}_{aL}\gamma^\lambda\psi_{bL}\rangle\bar{\psi}_{cL}\gamma_\lambda\psi_{dL}+\bar{\psi}_{aL}\gamma^\lambda\psi_{dL}\langle\bar{\psi}_{cL}\gamma_\lambda\psi_{bL}\rangle\\&+\langle\bar{\psi}_{aL}\gamma^\lambda\psi_{dL}\rangle\bar{\psi}_{cL}\gamma_\lambda\psi_{bL}-\langle\bar{\psi}_{aL}\gamma^\lambda\psi_{bL}\rangle\langle\bar{\psi}_{cL}\gamma_\lambda\psi_{dL}\rangle-\langle\bar{\psi}_{aL}\gamma^\lambda\psi_{dL}\rangle\langle\bar{\psi}_{cL}\gamma_\lambda\psi_{bL}\rangle\ ,\end{aligned} \tag{2.6}$$

where ψ_a, ψ_b, ψ_c, and ψ_d are arbitrary fermion fields. Equation (2.6) is like a Hartree-Fock approximation. The first two terms, the "diagonal terms," are the "Hartree" part of a Hartree-Fock approximation. The third and fourth terms are "exchange interactions" and enter additively because of Fermi statistics. The last two terms in Eq. (2.6) do not lead to interactions; they contribute to the vacuum energy and comprise the "constant" in Eq. (2.5).

The second subtlety is that the off-diagonal backgrounds $\langle\bar{\nu}_{eL}\gamma^\lambda\nu_{\mu L}\rangle$ and $\langle\bar{\nu}_{\mu L}\gamma^\lambda\nu_{eL}\rangle$ cannot be set to zero, in contrast with the case of massless neutrinos. When mixing is present, $\langle\bar{\nu}_{eL}\gamma^\lambda\nu_{\mu L}\rangle$ and $\langle\bar{\nu}_{\mu L}\gamma^\lambda\nu_{eL}\rangle$ are generally nonzero. Even when they vanish at time $t=0$, they usually are not zero for later times. In certain situations, off-diagonal backgrounds vanish in the mass-eigenstate basis. However, if they vanish in that basis, a simple calculation shows that they do not vanish in the flavor basis. The examples in Sec. IV illustrate the need to keep off-diagonal backgrounds.

The above two subtleties were discussed by Pantaleone in Refs. [13,14]. Previous treatments of neutrino gases often did not properly take these effects into account.

B. The self-interacting system

A dense neutrino gas is a complicated system. The propagation of a particular neutrino depends on its interaction with the other leptons. Since neutrinos oscillate, the nature of the lepton background is continually changing. Furthermore, unlike the case of electrons in the Sun, where the electron density is known to high precision, the background neutrino densities are *a priori* not known but must be calculated. One must know the neutrino background to determine how an individual neutrino oscillates, but one must know the flavor of every individual neutrino to determine the background. A brute force approach treats the coupled system in its entirety and would require tremendous computing capabilities. However, when the number of neutrinos is large, the methods of statistical mechanics are applicable and a simplification is expected to occur.

Let $\nu^{(i)}(\mathbf{x},t)$ denote the wave function for the ith neutrino. In flavor space, we write

$$\nu^{(i)}(\mathbf{x},t)=\begin{bmatrix}\nu_e^{(i)}(\mathbf{x},t)\\ \nu_\mu^{(i)}(\mathbf{x},t)\end{bmatrix}\ , \tag{2.7}$$

where $\nu_e^{(i)}$ and $\nu_\mu^{(i)}$ are the electron-neutrino and muon-neutrino components. The wave function satisfies the normalization condition

$$\int d^3x\, \nu_e^{(i)\dagger}(\mathbf{x},t)\nu_e^{(i)}(\mathbf{x},t)+\int d^3x\, \nu_\mu^{(i)\dagger}(\mathbf{x},t)\nu_\mu^{(i)}(\mathbf{x},t)=1\ . \tag{2.8}$$

The two terms in Eq. (2.8) are, respectively, the probability that the ith neutrino is an electron neutrino and a muon neutrino at time t. If the ith particle happens to be an antineutrino, the wave function is normalized to -1 instead of $+1$ in Eq. (2.8). In Eqs. (2.7) and (2.8) and henceforth, the Dirac indices on $\nu^{(i)}(\mathbf{x},t)$ are not displayed.

The wave function $\nu^{(i)}(\mathbf{x},t)$ is the solution to the Dirac equation with interactions given in Eqs. (2.3) and (2.5) where the neutrino background are

$$\begin{aligned}
\langle \bar\nu_{eL}\gamma^\lambda\nu_{eL}\rangle(\mathbf{x},t)&=\sum_{j\neq i}\bar\nu_{eL}^{(j)}\gamma^\lambda\nu_{eL}^{(j)}(\mathbf{x},t)\ ,\\
\langle \bar\nu_{\mu L}\gamma^\lambda\nu_{\mu L}\rangle&=\sum_{j\neq i}\bar\nu_{\mu L}^{(j)}\gamma^\lambda\nu_{\mu L}^{(j)}(\mathbf{x},t)\ ,\\
\langle \bar\nu_{eL}\gamma^\lambda\nu_{\mu L}\rangle&=\sum_{j\neq i}\bar\nu_{eL}^{(j)}\gamma^\lambda\nu_{\mu L}^{(j)}(\mathbf{x},t)\ ,\\
\langle \bar\nu_{\mu L}\gamma^\lambda\nu_{eL}\rangle&=\sum_{j\neq i}\bar\nu_{\mu L}^{(j)}\gamma^\lambda\nu_{eL}^{(j)}(\mathbf{x},t)\ .
\end{aligned} \tag{2.9}$$

The neutrino gas problem is highly nonlinear: The individual solutions $\nu^{(i)}(\mathbf{x},t)$ are obtained in the presence of the backgrounds in Eq. (2.9), yet these backgrounds are computed from the individual wave functions $\nu^{(i)}(\mathbf{x},t)$. This leads to a situation where a bootstrap approach is often necessary.

C. Symmetry and simplification

In practice, the system of interest has symmetries which simplify the analysis when statistical mechanics methods are employed. For example, consider a homogeneous gas in a large box of volume V. Then, only the temporal components of the background lepton currents, $J_L^\lambda(\mathbf{x},t)$, in Eqs. (2.3) and (2.9) are nonzero on average. One can use the replacements

$$J_L^\lambda(\mathbf{x},t)\to\delta_0^\lambda J_L^0(t)\equiv\frac{\delta_0^\lambda}{V}\int_V d^3x\, J_L^0(\mathbf{x},t)\ . \tag{2.10}$$

Thus, the backgrounds depend only on time and not position. In Eq. (2.10), J_L^λ stands for either $\langle \bar e_L\gamma^\lambda e_L\rangle$, $\langle \bar\mu_L\gamma^\lambda\mu_L\rangle$, $\langle \bar\nu_{eL}\gamma^\lambda\nu_{eL}\rangle$, $\langle \bar\nu_{\mu L}\gamma^\lambda\nu_{\mu L}\rangle$, $\langle \bar\nu_{eL}\gamma^\lambda\nu_{\mu L}\rangle$, or $\langle \bar\nu_{\mu L}\gamma^\lambda\nu_{eL}\rangle$. The flavor-diagonal currents are number densities since

$$\begin{aligned}
\frac{1}{V}\int_V d^3x\langle \nu_{eL}^\dagger\nu_{eL}\rangle(\mathbf{x},t)&=\rho_{\nu_e}(t)-\rho_{\bar\nu_e}(t)\ ,\\
\frac{1}{V}\int_V d^3x\langle \nu_{\mu L}^\dagger\nu_{\nu L}\rangle(\mathbf{x},t)&=\rho_{\nu_\mu}(t)-\rho_{\bar\nu_\mu}(t)\ ,\\
\frac{1}{V}\int_V d^3x\langle e_L^\dagger e_L\rangle(\mathbf{x},t)&=\rho_{e_L^-}(t)-\rho_{e_L^+}(t)\\
&\approx\frac{1}{2}[\rho_{e^-}(t)-\rho_{e^+}(t)]\ ,\\
\frac{1}{V}\int_V d^3x\langle \mu_L^\dagger\mu_L\rangle(\mathbf{x},t)&=\rho_{\mu_L^-}(t)-\rho_{\mu_L^+}(t)\\
&\approx\frac{1}{2}[\rho_{\mu^-}(t)-\rho_{\mu^+}(t)]\ .
\end{aligned} \tag{2.11}$$

In the last two equations, strict equality holds in the nonrelativistic limit.

For a system with spherical symmetry, as might occur in a supernova or a neutron star, the temporal and radial components of background currents are nonzero and depend on two variables, time and radial distance. In such a situation, an angular averaging is performed.

D. Calculational procedure

We assume certain information is exactly known such as background charged-lepton currents, initial neutrino backgrounds, initial individual wave functions, and the energy distribution of neutrinos. In principle, one should also know the fluctuations, both in space and time, of background densities. As a neutrino propagates through the medium there are regions with lepton densities that are slightly higher than and slightly lower than average densities. Such variations slightly affect the oscillations of a neutrino.

If a "neutrino detector" is placed in the gas, the time resolution of the detector must be known. If the measurement takes several oscillation times, an averaging over this time scale must be made. A similar procedure might be necessary initially, if background neutrino currents are not known for $t=0$. It could be that the neutrinos are generated over a period of time, in which case, the initial production profile must be supplied.

In summary, there are probability distributions governing a gas and representing intrinsic uncertainties. These distributions must be *a priori* known. Important physics is often encoded in the probability distributions.

A solution to the neutrino gas problem is a specification of the background neutrino currents for $t\geq 0$ satisfying two requirements. (i) The solution must agree with initial conditions and be continuous. (ii) A consistency condition must be satisfied. After obtaining the wave functions $\nu^{(i)}(\mathbf{x},t)$ from the Dirac equation in the presence of background currents, the background neutrino currents, as computed from the $\nu^{(i)}(\mathbf{x},t)$ in Eq. (2.9), must agree with the backgrounds originally proposed. In checking this, one must average over the uncertainties given in the previous paragraphs. In other words, wave functions must be computed for varying energies, different propagation times, fluctuations in backgrounds, and various initial conditions. The averaging over these uncertainties is performed with *a priori* known distributions. In certain situations, the self-consistency condition is automatically satisfied; however, in some circumstances considerable effort is required.

One way to find neutrino background solutions is as follows. An educated initial guess for backgrounds is made. Then, individual wave functions $\nu^{(i)}(\mathbf{x},t)$ are computed. From these, an output background via Eq. (2.9) is computed and a modified background is proposed. A way of choosing the modified background is to let it be a linear combination of input and output backgrounds. One then repeats the procedure until the self-consistency condition is met. In essence, one is trying to find a fixed point in a multivariable space. Standard methods to deal with such problems can be employed.

III. THE SPATIALLY HOMOGENEOUS CASE

A. Evolution equation for an individual neutrino

This section treats the spatially homogeneous gas. Equations (2.10) and (2.11) are valid; only temporal components of currents are nonzero and they are independent of position. We assume that vacuum and matter-induced neutrino masses are much smaller than the neutrino's energy E so that the neutrinos are relativistic. We also assume that forward scattering dominates and higher-order processes can be neglected, i.e., $G_F E^2 \ll 1$.

Under these conditions, it is valid to linearize the Dirac equation in the standard manner [15] as

$$4Ei\frac{d}{dt}\nu = \text{const} \times \begin{bmatrix} 1 & 0 \\ 0 & 1 \end{bmatrix} \nu + 4Eh\nu \ , \tag{3.1}$$

where

$$\nu = \begin{bmatrix} \nu_{eL} \\ \nu_{\mu L} \end{bmatrix}$$

and h acts like a time-dependent Hamiltonian:

$$4Eh = \begin{bmatrix} B + A - \Delta\cos(2\theta_v) & \Delta\sin(2\theta_v) + B_{\mu e} \\ \Delta\sin(2\theta_v) + B_{e\mu} & -B - A + \Delta\cos(2\theta_v) \end{bmatrix} . \tag{3.2}$$

Since we are considering a specific neutrino, we drop a superscript (i) on ν, E, and h for convenience. In Eq. (3.2), θ_v is the vacuum mixing angle which relates the flavor basis, ν_e and ν_μ, to the vacuum mass-eigenstate basis, ν_1 and ν_2, via

$$\begin{bmatrix} \nu_1 \\ \nu_2 \end{bmatrix} = \begin{bmatrix} \cos(\theta_v) & -\sin(\theta_v) \\ \sin(\theta_v) & \cos(\theta_v) \end{bmatrix} \begin{bmatrix} \nu_{eL} \\ \nu_{\mu L} \end{bmatrix} . \tag{3.3}$$

The difference Δ of the square of the vacuum masses m_1 and m_2 is

$$\Delta = m_2^2 - m_1^2 \ . \tag{3.4}$$

The charged-lepton-induced mass-squared difference A is given by

$$\begin{aligned} \frac{A}{2\sqrt{2}G_F E} &= 2(\langle e_L^\dagger e_L \rangle - \langle \mu_L^\dagger \mu_L \rangle) \\ &\approx \langle e^\dagger e \rangle - \langle \mu^\dagger \mu \rangle = [\rho_{e^-} - \rho_{e^+} - (\rho_{\mu^-} - \rho_{\mu^+})] \ , \end{aligned} \tag{3.5}$$

and the neutrino background densities are

$$\begin{aligned} \frac{B}{2\sqrt{2}G_F E} &= \langle \nu_{eL}^\dagger \nu_{eL} \rangle - \langle \nu_{\mu L}^\dagger \nu_{\mu L} \rangle \\ &= [\rho_{\nu_{eL}} - \rho_{\bar{\nu}_{eL}} - (\rho_{\nu_{\mu L}} - \rho_{\bar{\nu}_{\mu L}})] \ , \\ B_{\mu e} &= 4\sqrt{2}G_F E \langle \nu_{\mu L}^\dagger \nu_{eL} \rangle \ , \\ B_{e\mu} &= B_{\mu e}^\dagger = 4\sqrt{2}G_F E \langle \nu_{eL}^\dagger \nu_{\mu L} \rangle \ . \end{aligned} \tag{3.6}$$

The angular brackets represent an averaging procedure in Eq. (2.9) which arises from statistical distributions and fluctuations of the gas. In short, Eqs. (3.1)–(3.6) determine the evolution of a single neutrino.

It is useful to define some parameters associated with Eq. (3.2). The instantaneous matter-induced mass-eigenstate basis is obtained by diagonalizing h using a unitary matrix U_m via

$$h = U_m \begin{bmatrix} -\pi/\lambda_m & 0 \\ 0 & \pi/\lambda_m \end{bmatrix} U_m^\dagger \ , \tag{3.7}$$

where one can write

$$U_m = \begin{bmatrix} e^{i\alpha_m} & 0 \\ 0 & e^{-i\alpha_m} \end{bmatrix} \begin{bmatrix} \cos(\theta_m) & \sin(\theta_m) \\ -\sin(\theta_m) & \cos(\theta_m) \end{bmatrix} . \tag{3.8}$$

In general, this basis is time dependent since h and U_m depend on t. Unlike the MSW case when only an electron background is present, there is an additional angle α_m because the off-diagonal term $\Delta\sin(2\theta_v) + B_{e\mu}$ in h is generally complex:

$$2\alpha_m \equiv -\arg[\Delta\sin(2\theta_v) + B_{e\mu}] \ . \tag{3.9}$$

The matter-induced mixing angle θ_m is defined as

$$\tan(2\theta_m) \equiv \frac{|\Delta\sin(2\theta_v) + B_{e\mu}|}{-B - A + \Delta\cos(2\theta_v)} \ . \tag{3.10}$$

The matter-induced oscillation time (or length since we take $c = 1$) λ_m is

$$\lambda_m \equiv 4\pi E / \Delta_m \ , \tag{3.11}$$

where the instantaneous mass-squared difference Δ_m is

$$\begin{aligned} \Delta_m \equiv \{ &[-B - A + \Delta\cos(2\theta_v)]^2 \\ &+ |\Delta\sin(2\theta_v) + B_{e\mu}|^2 \}^{1/2} \ . \end{aligned} \tag{3.12}$$

The subscript m on the above parameters stands for "matter induced." These parameters generally depend on time.

When the charged-lepton background A is time independent, the dependence of A in h can be eliminated by going to an effective mass-squared difference Δ_{eff} and an effective mixing angle θ_{eff} where

$$\begin{aligned} \tan(2\theta_{\text{eff}}) &= \frac{\Delta\sin(2\theta_v)}{-A + \Delta\cos(2\theta_v)} \ , \\ \Delta_{\text{eff}} &= \{[-A + \Delta\cos(2\theta_v)]^2 + \Delta^2\sin^2(2\theta_v)\}^{1/2} \ . \end{aligned} \tag{3.13}$$

This follows from

$$\begin{aligned} -A + \Delta\cos(2\theta_v) &= \Delta_{\text{eff}}\cos(2\theta_{\text{eff}}) \ , \\ \Delta\sin(2\theta_v) &= \Delta_{\text{eff}}\sin(2\theta_{\text{eff}}) \ . \end{aligned} \tag{3.14}$$

However, since this transformation is different for neutrinos of different energy, A cannot be completely eliminated from the problem. For a monoenergetic gas, one can set A to zero without loss of generality. In what follows, we use θ to denote θ_v or θ_{eff} (whichever is relevant for an individual neutrino) but we use Δ to denote Δ_{eff} even when $A \neq 0$.

The procedure is as follows. For fixed input backgrounds B and $B_{e\mu}$ one solves Eq. (3.1) over the ranges for

which parameters, such as energy, propagation time, etc., vary. Then, output backgrounds are computed via Eq. (2.9). A solution is obtained if input and output backgrounds coincide.

B. Magnetic-field-like reformulation

For a particular neutrino we use lower case b and $b_{e\mu}$ to denote the analogue of the background-averaged B and $B_{e\mu}$. Define bilinears in fields using

$$\begin{aligned} &b(t)\equiv 2\sqrt{2}G_F E[\nu_{eL}^{\dagger}\nu_{eL}(t)-\nu_{\mu L}^{\dagger}\nu_{\mu L}(t)] , \\ &b_{e\mu}(t)\equiv 4\sqrt{2}G_F E\nu_{eL}^{\dagger}\nu_{\mu L}(t), \quad b_{\mu e}(t)\equiv b_{e\mu}(t)^{\dagger} . \end{aligned} \tag{3.15}$$

Then, Eq. (3.1) implies

$$\begin{aligned} 4iE\frac{db}{dt} &= [\Delta\sin(2\theta)+B_{\mu e}]b_{e\mu}-[\Delta\sin(2\theta)+B_{e\mu}]b_{\mu e} , \\ 2iE\frac{db_{e\mu}}{dt} &= [\Delta\sin(2\theta)+B_{e\mu}]b+[\Delta\cos(2\theta)-B]b_{e\mu} , \end{aligned} \tag{3.16}$$

as well as particle-number conservation which is expressed as

$$\frac{d[\nu_{eL}^{\dagger}\nu_{eL}(t)+\nu_{\mu L}^{\dagger}\nu_{\mu L}(t)]}{dt}=0 . \tag{3.17}$$

Let

$$\begin{aligned} &v_1\equiv b, \quad v_2\equiv \mathrm{Re}(b_{e\mu}), \quad v_3\equiv \mathrm{Im}(b_{e\mu}) , \\ &\mathbf{v}\equiv(v_1,v_2,v_3) . \end{aligned} \tag{3.18}$$

Then, Eq. (3.16) resembles the propagation of a particle in a magnetic field:

$$\frac{d\mathbf{v}}{dt}=\frac{\mathbf{v}\times\mathcal{B}}{2E} , \tag{3.19}$$

where e/m, charge over mass, is replaced by $1/(2E)$, and the magnetic field $\mathcal{B}$ has a fixed component $\mathcal{B}_0$ and a component $\langle\mathbf{v}\rangle$ generated from the neutrino background:

$$\begin{aligned} &\mathcal{B}\equiv-\langle\mathbf{v}\rangle+\mathcal{B}_0 , \\ &\mathcal{B}_0\equiv\Delta(\cos(2\theta),-\sin(2\theta),0) , \end{aligned} \tag{3.20}$$

where $\langle\mathbf{v}\rangle$ denotes the averaging procedure performed on $\mathbf{v}$.

The computation proceeds by solving Eq. (3.19) for varying parameters, then doing the averaging directly on $\mathbf{v}$, and finally requiring self-consistency. The formulation in Eq. (3.19) provides useful insight in understanding neutrino oscillations.

C. Dimensionless parameters

This subsection makes manifest the dependencies on various parameters. We do this by going to dimensionless quantities. The numerical simulations in Sec. IV are performed using the variables of this subsection.

For a particular neutrino, define a dimensionless wave function $\phi^{(i)}$ [(i) denotes the ith neutrino], a dimensionless time τ, and dimensionless backgrounds $\langle\beta\rangle$ and $\langle\beta_{e\mu}\rangle$ using

$$\begin{aligned} &\phi^{(i)}\equiv\sqrt{V}\,\nu^{(i)}, \quad \tau\equiv 2\sqrt{2}G_F\rho_\nu t , \\ &\langle\beta\rangle\equiv\frac{B}{2\sqrt{2}G_F E\rho_\nu}, \quad \langle\beta_{e\mu}\rangle\equiv\frac{B_{e\mu}}{2\sqrt{2}G_F E\rho_\nu} , \\ &\langle\beta_{\mu e}\rangle\equiv\langle\beta_{e\mu}^{\dagger}\rangle , \end{aligned} \tag{3.21}$$

where $\rho_\nu=(N_\nu-N_{\bar\nu})/V$ is the net neutrino density, $\rho_\nu=\rho_{\nu_e}+\rho_{\nu_\mu}-\rho_{\bar\nu_e}-\rho_{\bar\nu_\mu}$, and V is the volume of the gas. The bilinears $\beta^{(i)}$ and $\beta_{e\mu}^{(i)}$ are given in terms of $\phi^{(i)}$ without dimensionful constants via

$$\begin{aligned} &\beta^{(i)}=\phi_e^{(i)\dagger}\phi_e^{(i)}-\phi_\mu^{\dagger}\phi_\mu^{(i)}, \quad \beta_{e\mu}^{(i)}=2\phi_e^{(i)\dagger}\phi_\mu^{(i)} , \\ &(N_\nu-N_{\bar\nu})\langle\beta\rangle\equiv\sum_i\beta^{(i)}, \quad (N_\nu-N_{\bar\nu})\langle\beta_{e\mu}\rangle\equiv\sum_i\beta_{e\mu}^{(i)} . \end{aligned} \tag{3.22}$$

From Eqs. (3.16) and (3.21), one finds

$$4i\frac{d}{d\tau}\phi^{(i)}=\begin{bmatrix}\langle\beta\rangle-\kappa\cos(2\theta) & \kappa\sin(2\theta)+\langle\beta_{\mu e}\rangle \\ \kappa\sin(2\theta)+\langle\beta_{e\mu}\rangle & -\langle\beta\rangle+\kappa\cos(2\theta)\end{bmatrix}\phi^{(i)} , \tag{3.23}$$

where κ is the dimensionless parameter

$$\kappa\equiv\frac{\Delta}{2\sqrt{2}G_F E\rho_\nu} . \tag{3.24}$$

Neutrinos with different energies have different κ. For neutrinos with $\kappa\gg1$, the vacuum mass difference is much greater than the neutrino-induced mass and those neutrinos should oscillate in a manner similar to the vacuum case, unless subtle effects somehow lead to an amplification. When $\kappa\ll1$, the neutrino-induced mass is large and it is crucial to include neutrino backgrounds. Equations (3.23) and (3.24) show that the oscillation of a neutrino does not depend separately on Δ, E, and ρ_ν but in the combination given by κ. In dimensionless variables the magnetic-field-like reformation reads

$$\begin{aligned} &\hat{\mathbf{v}}\equiv\frac{V}{2\sqrt{2}G_F E}\mathbf{v}=(\beta,\mathrm{Re}(\beta_{e\mu}),\mathrm{Im}(\beta_{e\mu})) , \\ &\frac{d\hat{\mathbf{v}}}{d\tau}=\frac{1}{2}\hat{\mathbf{v}}\times\hat{\mathcal{B}}, \quad \hat{\mathcal{B}}=-\langle\hat{\mathbf{v}}\rangle+\hat{\mathcal{B}}_0 , \\ &\hat{\mathcal{B}}_0\equiv\kappa(\cos(2\theta),-\sin(2\theta),0) , \end{aligned} \tag{3.25}$$

where a caret indicates a dimensionless vector quantity.

Figure 1 illustrates the magnetic-field-like reformulation. If neutrino-neutrino interactions are neglected then $\hat{\mathcal{B}}=\hat{\mathcal{B}}_0$ and the vector $\hat{\mathbf{v}}(t)$ rotates around $\hat{\mathcal{B}}_0$. In general, $\langle\hat{\mathbf{v}}(t)\rangle\neq\hat{\mathbf{v}}(t)$ and neutrino self-interactions provide an additional contribution to the force in Eq. (3.19) given by $\langle\hat{\mathbf{v}}(t)\rangle\times\hat{\mathbf{v}}(t)/2$.

Using Fig. 1, one easily sees that our approach is basis

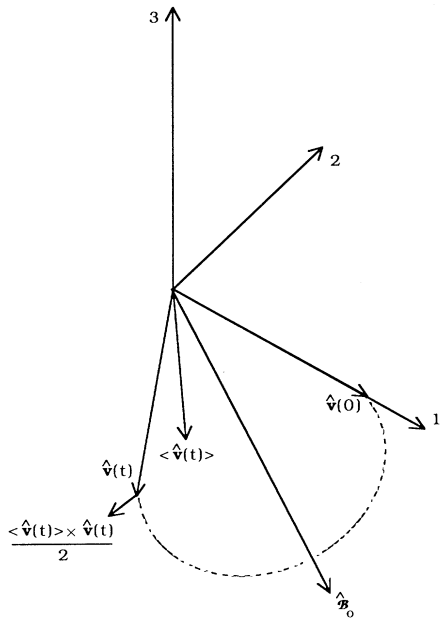

FIG. 1. The magnetic-field-like reformulation. The broken line shows the orbit of the vector $\hat{\mathbf{v}}(t)$ defined in Eq. (3.25). If $\hat{\mathbf{v}}(t)$ and $\langle\hat{\mathbf{v}}(\tau)\rangle$ are not parallel, then the neutrino background produces a force equal to $\langle\hat{\mathbf{v}}(\tau)\rangle\times\hat{\mathbf{v}}(\tau)/2$. When $\langle\hat{\mathbf{v}}(\tau)\rangle$ lags behind $\hat{\mathbf{v}}(t)$, this force causes $\hat{\mathbf{v}}(t)$ to spiral outward away from $\hat{\mathcal{B}}_0$ as indicated.

independent. A different basis simply orients the 1, 2, and 3 axes in Fig. 1 differently. However, the relative orientation of $\hat{\mathbf{v}}(0)$ and $\hat{\mathcal{B}}_0$ as well as the evolution of $\hat{\mathbf{v}}(t)$ and $\langle\hat{\mathbf{v}}(t)\rangle$ as determined from Eqs. (3.25) and (2.9) are unchanged.

In addition to κ and θ, neutrino oscillations depend on the parameters specifying the averaging procedure and entering in probability distributions. They also depend on the initial neutrino wave functions and backgrounds.

D. An adiabaticlike approximation

Because of the complicated nature of the dense neutrino gas problem, one must probably proceed numerically to obtain accurate results. For ordinary neutrino oscillations, approximate analytic methods exist [15]. One such method is the adiabatic approximation. In this subsection, we derive the analogue of this approximation for the neutrino gas.

Let $G(t_f,t_i)$ be the propagation matrix. It evolves a solution ν of Eq. (3.1) at time t_i to a solution at time t_f: $\nu(t_f)=G(t_f,t_i)\nu(t_i)$. For small δt,

$$G(t+\delta t,t)=\exp[-i\delta t h(t)] .$$

Using Eq. (3.7),

$$G(t+\delta t,t)=U_m(t)\begin{bmatrix} e^{[i\pi/\lambda_m(t)]\delta t} & 0 \\ 0 & e^{-[i\pi/\lambda_m(t)]\delta t}\end{bmatrix}U_m^\dagger(t) . \tag{3.26}$$

The full $G(t_f,t_i)$ is obtained by multiplying successive $G(t+\delta t,t)$. If

$$\lambda_m\frac{d\alpha_m}{dt}\ll 1 \quad\text{and}\quad \lambda_m\frac{d\theta_m}{dt}\ll 1 , \tag{3.27}$$

then, as a function of t, $U_m(t)$ varies slowly compared to the oscillating factor $\exp(i\pi\delta t/\lambda_m)$. Hence, when one multiplies successive $G(t+\delta t,t)$, the U_m at adjacent times cancel except for the first and last U_m. Denoting G_{aa} as the adiabatic approximation to G, one has

$$\begin{aligned} G(t_f,t_i)&\approx G_{aa}(t_f,t_i) \\ &\equiv U_m(t_f)\begin{bmatrix} e^{i\pi\varphi} & 0 \\ 0 & e^{-i\pi\varphi}\end{bmatrix}U_m^\dagger(t_i) ,\end{aligned} \tag{3.28}$$

where

$$\varphi=\int_{t_i}^{t_f}\frac{ds}{\lambda_m(s)} . \tag{3.29}$$

Let us use G_{aa} as the propagation matrix. From the solutions ν as determined from G_{aa}, one computes the bilinears b and $b_{e\mu}$ in Eq. (3.15). They are functions of $\exp(2i\pi\varphi)$. Assume that t_f-t_i is much bigger than any oscillation time. In computing B and $B_{e\mu}$ in terms of b and $b_{e\mu}$, statistical distributions are expected to produce variations in $\lambda_m(t)$ and hence large fluctuations in $\exp(2i\pi\varphi)$, which effectively set this phase factor to zero:

$$b|_{\exp(2\pi i\varphi)=0}\to B, \quad b_{e\mu}|_{\exp(2\pi i\varphi)=0}\to B_{e\mu} ,$$
$$\text{for } t_f-t_i\gg\lambda_m . \tag{3.30}$$

Straightforward but lengthy algebra gives B and $B_{e\mu}$ as

$$\begin{aligned} B(t_f)&=\langle b(t_f)\rangle \\ &=\langle c_{2f}c_{2i}b(t_i)\rangle-\mathrm{Re}[\langle c_{2f}s_{2i}e^{2i\alpha_m(t_i)}b_{e\mu}(t_i)\rangle] , \\ B_{e\mu}(t_f)&=-\langle e^{-2i\alpha_m(t_f)}\tan[2\theta_m(t_f)]b(t_f)\rangle ,\end{aligned} \tag{3.31}$$

where the abbreviations $c_{2i}=\cos[2\theta_m(t_i)]$, $s_{2i}=\sin[2\theta_m(t_i)]$, $c_{2f}=\cos[2\theta_m(t_f)]$, and $s_{2f}=\sin[2\theta_m(t_f)]$ are used.

The initial $\theta_m(t_i)$ and $\alpha_m(t_i)$ are determined from Eqs. (3.9) and (3.10). The final $\theta_m(t_f)$ and $\alpha_m(t_f)$ are found by using the results of Eq. (3.31) in Eqs. (3.9) and (3.10). In the case of a monoenergetic gas, $\theta_m(t)$ and $\alpha_m(t)$ are the same for all neutrinos and the factors depending on these angles in Eq. (3.31) can be taken outside the averaging brackets. Assuming a smooth asymptotic behavior, one then finds that $\alpha_m(t_f)$ is 0 or π. The two cases are

$$\tan[2\theta_m(t_f)]=\tan(2\theta) ,$$

when

$$e^{2i\alpha_m(t_f)}=1 \quad\text{and}\quad \Delta\sin(2\theta)+B_{e\mu}(t_f)>0 , \tag{3.32}$$

and

$$\tan[2\theta_m(t_f)]=-\tan(2\theta) ,$$

when

$$e^{2i\alpha_m(t_f)}=-1 \quad \text{and} \quad \Delta\sin(2\theta)+B_{e\mu}(t_f)<0 \ . \tag{3.33}$$

In either case,

$$B_{e\mu}(t_f)=-\tan(2\theta)B(t_f) \ , \tag{3.34}$$

and $B_{e\mu}(t_f)$ is real. Equation (3.34) implies that the off-diagonal terms in the mass eigenstate basis vanish for late times. This follows from

$$\begin{bmatrix} B^M \\ \mathrm{Re}(B^M_{e\mu}) \end{bmatrix} = \begin{bmatrix} \cos(2\theta) & -\sin(2\theta) \\ \sin(2\theta) & \cos(2\theta) \end{bmatrix} \begin{bmatrix} B \\ \mathrm{Re}(B_{e\mu}) \end{bmatrix} , \qquad \mathrm{Im}(B^M_{e\mu})=\mathrm{Im}(B_{e\mu}) \ , \tag{3.35}$$

where the superscript M indicates the asymptotic mass-eigenstate basis.

It is unclear when the adiabatic approximation can be used from $t_i=0$ to $t_f=\infty$. Unlike the MSW case of an electron background in which one can imagine a situation for which $\rho_e(r)$ varies very slowly with the distance r, the neutrino backgrounds tend to oscillate at the same rate as an individual neutrino, especially for early times for certain initial situations. Hence, the adiabatic approximation can hold only if the amplitudes of the neutrino backgrounds are small. Even in this case, the adiabatic approximation might break down if small effects add constructively over a long time period of time. Furthermore, the adiabatic approximation gives a result independent of the averaging prescription. In Sec. IV, we show that there can be sensitivity to the parameters in the statistical distributions. We also provide an example where, although Eqs. (3.27) are valid, the adiabatic approximation fails due to a parametric resonance [16,17].

Figure 2 displays the survival probability of electron neutrinos assuming that $\alpha(t_f)=0$ and assuming that the adiabatic approximation is valid for all times. Starting with a gas of electron neutrinos, oscillations convert some particles into muon neutrinos. Plotted in Fig. 2 are contours of constant survival probability P, i.e., the fraction of neutrinos that remains electron neutrinos as $t\to\infty$. The formula for P is

$$P=\tfrac{1}{2}+\tfrac{1}{2}\cos(2\theta)\cos[2\theta_m(0)] \ ,$$

where $\theta_m(0)$ is the initial matter-induced mixing angle:

$$\tan[2\theta_m(0)]=\sin(2\theta)/[-1/\kappa+\cos(2\theta)] \ .$$

Figure 2 provides a rough picture of neutrino-oscillation results in neutrino gases.

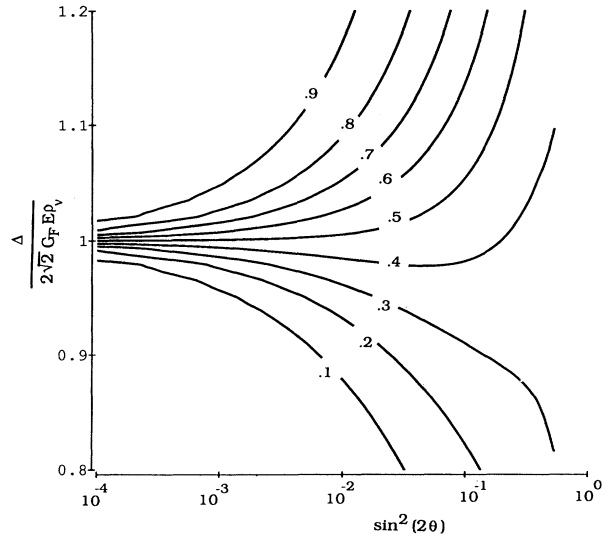

FIG. 2. The survival probability according to the adiabatic approximation. In this figure we assume that the adiabatic approximation is exact and that $\lim_{t\to\infty}2\alpha_m(t)=0 \bmod 2\pi$. Lines of constant survival probability P are shown as a function of $\sin^2(2\theta)$ and $\kappa=\Delta/2\sqrt{2}G_F E\rho_\nu$.

For most systems, one expects the statistical distributions to produce backgrounds which are smooth for large times. If the charged-lepton background A is time independent, $B(t)$ and $B_{e\mu}(t)$ should become constant as t gets big. The adiabatic approximation can then be used to take a result at a large time and extrapolate it to very large times. Hence, the result in Eq. (3.34) should hold generally. We now demonstrate this more rigorously.

E. Some general results

Assume $B(t)$ and $B_{e\mu}(t)$ have smooth limits as $t\to\infty$ and let t_f denote asymptotic late time. Apply the averaging procedure to Eq. (3.16). As $t\to\infty$, the left-hand side of Eq. (3.16) vanishes because, in averaging, b and $b_{e\mu}$ are replaced by $B(t)$ and $B_{e\mu}(t)$ which become constant. Therefore, the average of the right-hand side of Eq. (3.16) must be zero. This implies Eq. (3.34),

$$B_{e\mu}(t_f)=-\tan(2\theta)B(t_f) \ .$$

As $t\to\infty$, the background densities approach limits such that off-diagonal terms vanish in the mass eigenstate basis. There is a simple physical interpretation of this result via the magnetic-field reformation. The only preferred direction in Fig. 1 is along $\mathcal{B}_0$ so that if the backgrounds approach fixed values for large times, it should lie along the direction of $\mathcal{B}_0$. Since

$$\mathcal{B}_0 \propto (\cos(2\theta),-\sin(2\theta),0) \ ,$$

$$B_{e\mu}(t_f)=-\tan(2\theta)B(t_f) \ .$$

Secondly, a bound on $B(t_f)$ can be obtained. Since $\langle \mathbf{v}(t_f)\rangle$ points in the same direction as $\mathcal{B}_0$ and since $B(t_f)$ is the x-axis projection of $\langle \mathbf{v}(t_f)\rangle$,

$$-\cos(2\theta)\le\frac{B(t_f)}{2\sqrt{2}G_F E_{\max}\rho_\nu^{\text{total}}}\le\cos(2\theta) \ , \tag{3.36}$$

where $E_{\max}$ is the maximum energy of any neutrino and

$$\rho_\nu^{\text{total}}=(N_\nu+N_{\bar\nu})/V$$

is the total neutrino density. When $2\alpha_m(t_f)=0$ and $2\alpha_m(t_f)=\pi$, it is straightforward to show that the following holds for a monoenergetic gas:

$$\begin{aligned} &B(t_f)\le\Delta\cos(2\theta) \quad \text{when } 2\alpha_m(t_f)=0 \ , \\ &B(t_f)\ge\Delta\cos(2\theta) \quad \text{when } 2\alpha_m(t_f)=\pi \ . \end{aligned} \tag{3.37}$$

A third result concerns "a weak averaging procedure." If for some reason, $b(t)=B(t)$ and $b_{e\mu}(t)=B_{e\mu}(t)$, then the situation is that of a neutrinoless background. This follows from Eqs. (3.19) and (3.20). When $\mathbf{v}=\langle\mathbf{v}\rangle$, $\mathbf{v}\times\langle\mathbf{v}\rangle=0$ and the background-neutrino-induced magnetic-field term produces no effect. Consequently, one can replace $\mathcal{B}$ by $\mathcal{B}_0$ and neutrinos oscillate as if they were in a vacuum. For example, if only one neutrino is present in the gas, then $\mathbf{v}=\langle\mathbf{v}\rangle$ and this is the situation. If the spread in probability distributions is very narrow, one expects only small deviations from vacuum oscillation results.

IV. SAMPLE SIMULATIONS

To illustrate our ideas, we have performed exploratory numerical simulations for a gas of neutrinos with $N_{\bar{\nu}}=0$ (no antineutrinos). Solutions to Eq. (3.23) were obtained by numerical integration with a computer. The self-consistency condition, when it was not automatically satisfied, was implemented by an iterative procedure. We have performed enough numerical work to gain some insight into the physics of dense neutrino gases. However, our studies are not exhaustive and further work is needed.

For reasons of space, we discuss selected examples; significantly more simulations have been performed. We observed several interesting effects. With one exception, neutrino oscillations resemble, as expected, the vacuum case, when the neutrino gas is not too dense. In the exceptional case, a parametric resonant conversion of neutrinos occurred; a gas of electron neutrinos, although dilute, was able to slowly convert into a gas of predominantly muon neutrinos. It took many many oscillation times for this to happen. When the neutrino gas is dense, we find that a self-induced resonant conversion can occur. Most electron neutrinos are converted into muon neutrinos. In an exceptional case, an unusual cooperative phenomenon occurred in which neutrinos oscillated more or less in phase. An averaging procedure failed to produce incoherence. The self-maintained coherence arose for a situation in which one expected incoherence.

A general result concerns initial conditions. If all neutrinos are initially in mass eigenstates then there are no oscillations. To show this, note that all

$$b_{e\mu}(0)=-\tan(2\theta)b(0)$$

and consequently

$$B_{e\mu}(0)=-\tan(2\theta)B(0)\ .$$

Next, note that the time derivatives db/dt and $db_{e\mu}/dt$ are zero at $t=0$ since the right-hand side of Eq. (3.16) vanishes. For each neutrino, let $b(t)=b(0)$ and $b_{e\mu}(t)=b_{e\mu}(0)$ be the constant solution. Then $B(t)=b(0)$ and $B_{e\mu}(t)=b_{e\mu}(0)$ also because the average of a constant is *the* constant. Hence $B_{e\mu}=-\tan(2\theta)B$ for all times. A solution is found since both sides of Eq. (3.16) are zero.

We used two generic types of averaging procedures: time averaging and energy averaging. The latter is necessary in any physical gas since neutrinos will have an energy distribution. To simulate the system we used many neutrinos with different energies. In doing so, the self-consistency condition is implemented automatically since backgrounds can be determined by averaging over the various wave functions. Time averaging is less physical but is expected to produce effects similar to more realistic systems. It is also presented to illustrate the self-consistency condition.

The numerical simulations were performed using the dimensionless parameters of Sec. III C. Initially, all neutrinos were taken to be electron neutrinos, i.e.,

$$\hat{\mathbf{v}}(0)=\langle\hat{\mathbf{v}}(0)\rangle=(1,0,0)\ ,$$

cf. Eq. (3.25). Although other values of $\sin^2(2\theta)$ were simulated, we use $\sin^2(2\theta)=0.25$ for all the numerical examples presented below.

A. General comments on time-averaging procedures

Given a solution $\hat{\mathbf{v}}$ of Eq. (3.25), we define the time-averaged background $\langle\hat{\mathbf{v}}\rangle$ to be

$$\langle\hat{\mathbf{v}}(\tau)\rangle=\frac{1}{\tau(f_m+f_p)}\int_{\tau(1-f_m)}^{\tau(1+f_p)}d\sigma\,\hat{\mathbf{v}}(\sigma)\ , \tag{4.1}$$

where

$$\hat{\mathbf{v}}=(\beta,\mathrm{Re}(\beta_{e\mu}),\mathrm{Im}(\beta_{e\mu}))$$

and f_m and f_p are the backward and forward time-averaging fractions. The physical motivation for time averaging is that various effects cause different neutrinos to propagate for different amount of time. The solution $\hat{\mathbf{v}}(\sigma)$ can represent any one of the neutrinos. By time averaging, one implements the idea of different times of flight. The advantage of this approach is that only one solution of Eq. (3.25) need be known. A flat distribution is used in Eq. (4.1); if desired, one can use another distribution. Since the averaging time interval increases without limit as $\tau\to\infty$, one expects the backgrounds to go to smooth limits. Indeed, from Eq. (4.1) one can show that

$$\left|\frac{d\langle\hat{\mathbf{v}}\rangle}{d\tau}\right|<\frac{\text{const}}{\tau}\to 0$$

as $\tau\to\infty$. Time averaging guarantees that neutrinos interfere incoherently. In Sec. IV B, we consider symmetric-time averaging for which $f_m=f_p$. In Sec. IV C, we treat backward-time averaging for which $f_p=0$.

For small times, one can obtain accurate analytical results for $\hat{\mathbf{v}}(\tau)$ and $\langle\hat{\mathbf{v}}(\tau)\rangle$ by performing a Taylor-series expansion in τ. The results are presented in the Appendix. We used series with up to ten terms to verify our numerical simulations in the small τ region.

The time-averaging procedure illustrates well the self-consistency condition. A background $\langle\hat{\mathbf{v}}\rangle$ is a solution if $\langle\hat{\mathbf{v}}\rangle$ is the result of time averaging over $\hat{\mathbf{v}}(\sigma)$ in Eq. (4.1) when $\hat{\mathbf{v}}(\tau)$ is obtained by integrating Eq. (3.25) using $\langle\hat{\mathbf{v}}\rangle$ as the background. In practice, we found such background solutions by iteration. An initial background $\langle\hat{\mathbf{v}}\rangle_{\text{in}}$ was proposed. Using $\langle\hat{\mathbf{v}}\rangle_{\text{in}}$ for $\langle\hat{\mathbf{v}}\rangle$, Eq. (3.25) was solved by numerical integration on a computer. Then Eq.

(4.1) was used to generate an output $\langle \hat{\nu} \rangle_{\text{out}}$. The new background $\langle \hat{\nu} \rangle_{\text{new}}$ was selected as a weighted combination of $\langle \hat{\nu} \rangle_{\text{in}}$ and $\langle \hat{\nu} \rangle_{\text{out}}$ and used as the new initial input. The procedure was repeated until input and output backgrounds agreed.

B. Symmetric-time-averaging examples

The iterative procedure converged in the region $\kappa > 1$. As an example, consider 50% time averaging, i.e., $f_m = f_p = 0.5$, $\sin^2(2\theta) = 0.25$ and

$$\kappa = \Delta / 2\sqrt{2} G_F E \rho_\nu = 5.0 \ .$$

The large value of κ means that the mass difference induced by the neutrino background is much smaller than the vacuum mass difference. Hence, one expects neutrino oscillations to differ only slightly from the vacuum case and this indeed happens. Figures 3(a), 3(b), and 3(c) display the dimensionless backgrounds as a function of dimensionless time τ. The numerical asymptotic values are

$$\langle \beta \rangle \approx 0.753, \quad \langle \mathrm{Re}(\beta_{e\mu}) \rangle \approx -0.436 \ ,$$

and

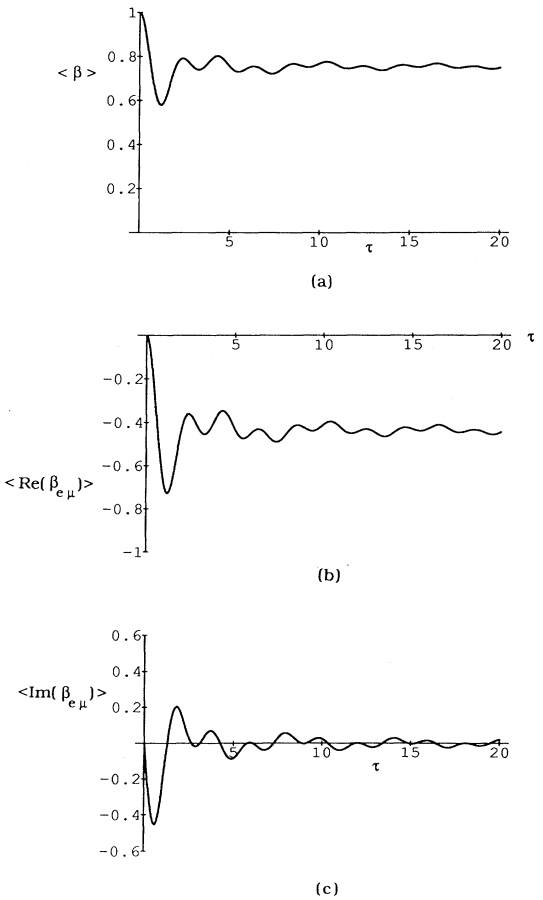

FIG. 3. The neutrino backgrounds as a function of time for a low-density neutrino gas with symmetric-time averaging. $\kappa = 0.5$, $\sin^2(2\theta) = 0.25$, and $f_m = f_p = 0.5$.

$$\langle \mathrm{Im}(\beta_{e\mu}) \rangle \approx 0.000 \ .$$

In the absence of background neutrinos, i.e., vacuum oscillations, the asymptotic values would be

$$\langle \beta \rangle = \cos^2(2\theta) = 0.75 \ ,$$

$$\langle \mathrm{Re}(\beta_{e\mu}) \rangle = -\sin(2\theta)\cos(2\theta) \approx -0.433 \ ,$$

and $\langle \mathrm{Im}(\beta_{e\mu}) \rangle = 0$. These vacuum values are close to the numerical results. The adiabatic predictions of

$$\langle \beta \rangle \approx 0.693, \quad \langle \mathrm{Re}(\beta_{e\mu}) \rangle \approx -0.400 \ ,$$

and

$$\langle \mathrm{Im}(\beta_{e\mu}) \rangle \approx 0.000$$

from Eq. (3.31) are in less agreement, suggesting that the system behaves more like the vacuum than expected. The prediction of

$$\langle \mathrm{Re}(\beta_{e\mu}) \rangle / \langle \beta \rangle = -\tan(2\theta) \approx -0.577$$

in Eq. (3.34) is confirmed. Our numerical result is

$$\langle \mathrm{Re}(\beta_{e\mu}) \rangle / \langle \beta \rangle \approx -0.579 \ .$$

The other values of $\sin^2(2\theta)$ for $\kappa > 1$ which we examined produced results which also mimicked vacuum behavior for neutrino oscillations.

When $\kappa < 1$ and the neutrino gas is dense, we were unable to find the backgrounds for all times using the above-mentioned iterative procedure. Nevertheless, some conclusions can be drawn. In a simulation with parameters in the previous example except $\kappa = 0.5$, we obtained the backgrounds to a few percent for $\tau < 10$. Figure 4(a) displays $\langle \beta \rangle$ for $\tau < 20$. For $10 < \tau < 20$, the iterative procedure progressively broke down so that only $\sim 15\%$ accuracy was achieved. For $\tau > 20$, we were unable to determine the solution; however, examination of computer runs suggest that $\langle \beta \rangle$ continues to decrease and approaches 0.1 ± 0.3, meaning that almost 50% of electron neutrinos are converted into muon neutrinos.

It appears that there is a neutrino-self-induced MSW effect. In the absence of neutrino interactions, $\langle \beta \rangle = \cos^2(2\theta) = 0.75$. Numerical results give a considerably smaller value of $\langle \beta \rangle$. At $\tau = 0$, when all neutrinos are electron neutrinos, the matter-induced mixing angle θ_m in Eq. (3.10) is large and near $\pi/2$. As the neutrinos convert into muon neutrinos, $\langle \beta \rangle$ becomes smaller and θ_m decreases below $\pi/4$ as Fig. 4(b) shows. The situation is similar to the MSW resonant conversion of solar neutrinos created by a background electron density [2,3]. The differences are that, in our case, the electrons are replaced by the neutrinos themselves and time plays the role of distance from the Sun's center. Other values of $\sin^2(2\theta)$ give similar results, indicating that a self-induced MSW effect occurs for $\kappa < 1$.

C. Numerical simulations with back-time averaging

One can avoid the problem of iterative convergence by using back-time averaging. If $f_p = 0$, then the averaging procedure in Eq. (4.1) involves only earlier times. As-

sume that the wave function is numerically known up to time τ. The backgrounds at time τ are then determined from earlier values of the wave function and can be used to numerically integrate the wave functions from time τ to time $\tau+\Delta\tau$. By repeating the process, we obtain the backgrounds at all times. Although less interesting physically, back-time averaging provides no difficulties in satisfying the self-consistency conditions and is computationally simple.

Let us reconsider the last example for which $\sin^2(2\theta)=0.25$ and

$$\kappa=\Delta/2\sqrt{2}G_F E\rho_\nu=0.5 \ .$$

We use 50% back-time averaging: $f_m=0.5$. Figure 5(a) shows the electron-neutrino survival probability $P=(1+\langle\beta\rangle)/2$ as a function of time τ. There is almost complete conversion of electron neutrinos into muon neutrinos. Although electron neutrinos are quickly transformed into muon neutrinos, it actually takes a relatively long time interval to achieve asymptotic values for the backgrounds. Backgrounds are within a couple percent of asymptotic values when $\tau\approx 300$. Maximal conversion occurs, i.e.,

$$\lim_{\tau\to\infty}\langle P(\tau)\rangle=[1-\cos(2\theta)]/2\approx 0.067 \ .$$

A self-induced MSW effect has occurred. Figure 5(b) shows that the matter-induced mixing angle θ_m goes from a value near $\pi/2$ to a value near 0 as τ goes from 0 to ∞, just as in the MSW effect.

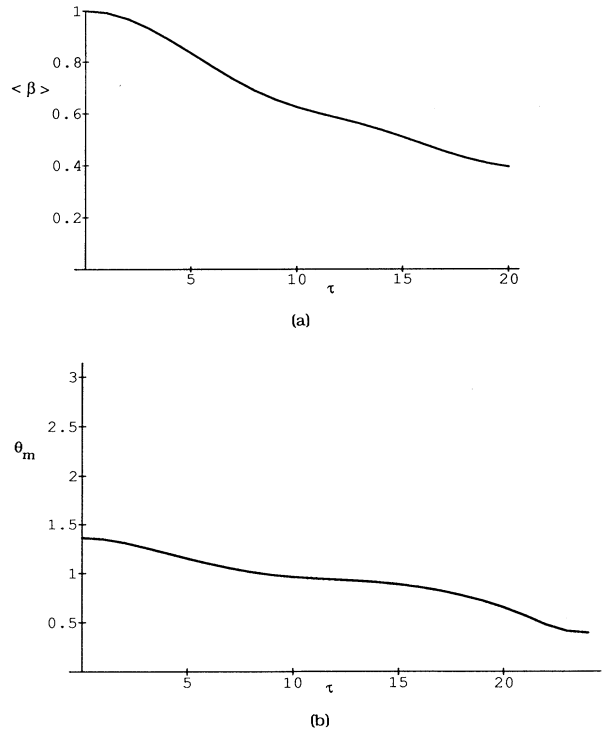

FIG. 4. The behavior for early times of a high-density neutrino gas with symmetric-time averaging. The results are for the same parameters as in Fig. 3 except $\kappa=5.0$.

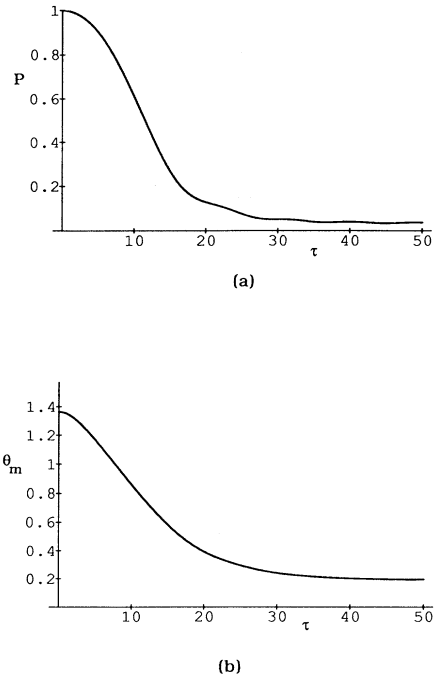

FIG. 5. The behavior of a dense neutrino gas with back-time averaging. The simulation is done with $\kappa=5.0$, $\sin^2(2\theta)=0.25$, $f_m=0.5$, and $f_p=0$.

Next, let us simulate a gas with a small background neutrino density. We use the parameters in the last example except for $\kappa=5.0$. For such a value of κ, one expects results similar to the vacuum case. Surprisingly, maximal conversion still occurs,

$$\lim_{\tau\to\infty}\langle\beta(\tau)\rangle=-\cos(2\theta)\approx -0.866 \ .$$

To analyze the physics, let us use the magnetic-field analogy given in Sec. III B. Figure 6 shows the orbit of $\hat{\mathbf{v}}(\tau)$ during the first eight or so oscillation times. At $\tau=0$, $\hat{\mathbf{v}}(\tau)=(1,0,0)$. The vector $\hat{\mathbf{v}}$ begins to precess around

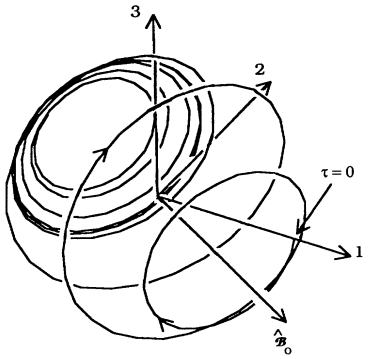

FIG. 6. The orbit of $\hat{\mathbf{v}}(\tau)$ for back-time averaging for the low-density gas of Fig. 5. The vector $\hat{\mathbf{v}}(\tau)$ begins at (1,0,0) and starts to circle around $\hat{\mathcal{B}}_0$. The background neutrinos, however, cause it to spiral backward and to eventually circle about $-\hat{\mathcal{B}}_0/\kappa$.

$$\hat{\mathcal{B}}_0=\kappa(\cos(2\theta),-\sin(2\theta),0)$$

and then gradually "spirals backward": $\hat{\mathbf{v}}_\parallel$, the component of $\hat{\mathbf{v}}$ parallel to $\hat{\mathcal{B}}_0$, decreases until $\hat{\mathbf{v}}$ points opposite to $\hat{\mathcal{B}}_0$. For large times, $\hat{\mathbf{v}}$ orbits in small circles about $-\hat{\mathcal{B}}_0/\kappa$. The asymptotic result is

$$\lim_{\tau\to\infty}\hat{\mathbf{v}}(\tau)=(-\cos(2\theta),\sin(2\theta),0)=\lim_{\tau\to\infty}\langle\hat{\mathbf{v}}(\tau)\rangle\ .$$

It takes many, many oscillation times to achieve the asymptotic value.

A parametric resonance has occurred. The neutrino background oscillates, more or less, in phase with an individual neutrino. Of course, time averaging reduces the amplitude of the background. The background is able to decrease $\hat{\mathbf{v}}_\parallel$ a little during each oscillation period. Without neutrino interactions, $\hat{\mathbf{v}}(\tau)$ circles around $\hat{\mathcal{B}}_0/\kappa$. With back-time averaging, $\langle\hat{\mathbf{v}}(\tau)\rangle$ "lags" behind $\hat{\mathbf{v}}(\tau)$. The effect of the neutrino background is to produce a force $\langle\hat{\mathbf{v}}(\tau)\rangle\times\hat{\mathbf{v}}(\tau)/2$. See Eq. (3.25). Figure 1 displays $\hat{\mathbf{v}}(\tau)$, $\langle\hat{\mathbf{v}}(\tau)\rangle$, and $\langle\hat{\mathbf{v}}(\tau)\rangle\times\hat{\mathbf{v}}(\tau)/2$. One observes that $\langle\hat{\mathbf{v}}(\tau)\rangle\times\hat{\mathbf{v}}(\tau)/2$ causes $\hat{\mathbf{v}}(\tau)$ to spiral backward; i.e., it makes $\hat{\mathbf{v}}_\parallel(\tau)$ decrease. Eventually it pushes $\hat{\mathbf{v}}(\tau)$ to $-\hat{\mathcal{B}}_0/\kappa$.

The above argument suggests that maximum conversion occurs for any θ, κ, and $f_m>0$ when $f_p=0$. We have numerically checked this for a number of simulations. For bigger κ and smaller f_m considerably more oscillation times are needed to achieve maximum conversion. The final result is

$$\lim_{\tau\to\infty}\langle\hat{\mathbf{v}}(\tau)\rangle=(-\cos(2\theta),\sin(2\theta),0)$$

(back-time averaging) (4.2)

for all the cases we have examined. Equation (4.2) saturates the lower bound in Eq. (3.36).

The above argument also suggests that, for forward-time averaging, the orbit should spiral forward and minimum conversion should occur. Using an iterative procedure to obtain the self-consistent backgrounds, we found

$$\lim_{\tau\to\infty}\langle\hat{\mathbf{v}}(\tau)\rangle=(\cos(2\theta),-\sin(2\theta),0)$$

(forward-time averaging) (4.3)

for all the cases we studied.

D. General results concerning averaging over an energy distribution

The particles in any physical gas have different energies. To deal with realistic neutrino gases, it is necessary to average over the energy distribution of the neutrinos. From Eqs. (3.22) to (3.24), one realizes that changing the neutrino energy E is equivalent to changing κ, but leaving β and $\beta_{e\mu}$ unchanged. A distribution in E corresponds to a distribution in $1/\kappa$. Unlike the time-averaging case, a constant charged-lepton background A cannot be eliminated by going to effective parameters because the transformation in Eq. (3.14) varies with energy and hence varies from neutrino to neutrino. In this and the next subsection, we set A to zero.

For energy averaging, the self-consistency condition is automatically satisfied. However, numerical integrations of many neutrino solutions must be computed. The procedure is as follows. Let there be N_ν neutrinos with wave functions $\phi^{(i)}$ and energies $E^{(i)}$, $i=1,\ldots,N_\nu$. Assume $\phi^{(i)}$ has been numerically computed up to time τ. Then, using Eq. (3.22), the backgrounds can be calculated by averaging over $\beta^{(i)}$ and $\beta_{e\mu}^{(i)}$. With $\langle\beta\rangle$ and $\langle\beta_{e\mu}\rangle$, one can numerically integrate to get the $\phi^{(i)}$ at $\tau+\Delta\tau$. The procedure is then repeated.

As in the case of time averaging, closed forms for the Taylor series in τ for

$$\hat{\mathbf{v}}^{(i)}=(\beta^{(i)},\mathrm{Re}(\beta_{e\mu}^{(i)}),\mathrm{Im}(\beta_{e\mu}^{(i)}))$$

and $\langle\hat{\mathbf{v}}\rangle$ can be obtained. An inductive algorithm is given in the Appendix. We uses such series to check computer programs.

For an energy-averaging procedure, neutrino particle numbers for mass eigenstates are conserved [13]. Let $\hat{\mathbf{v}}_\perp$ and $\hat{\mathbf{v}}_\parallel$ denote the components of $\hat{\mathbf{v}}$ perpendicular to and parallel to $\hat{\mathcal{B}}_0$. In terms of these components, Eq. (3.25) reads

$$2\frac{d\hat{\mathbf{v}}_\parallel(\tau)}{d\tau}=\langle\hat{\mathbf{v}}_\perp(\tau)\rangle\times\hat{\mathbf{v}}_\perp(\tau)\ , \tag{4.4}$$

$$2\frac{d\hat{\mathbf{v}}_\perp(\tau)}{d\tau}=\hat{\mathbf{v}}_\perp(\tau)\times\hat{\mathcal{B}}_0+\langle\hat{\mathbf{v}}_\perp(\tau)\rangle\times\hat{\mathbf{v}}_\parallel(\tau)+\langle\hat{\mathbf{v}}_\parallel\rangle\times\hat{\mathbf{v}}_\perp(\tau)\ . \tag{4.5}$$

Since Eq. (4.4) does not depend on a neutrino's energy, application of the averaging procedure to Eq. (4.4) yields

$$\frac{d\langle\hat{\mathbf{v}}_\parallel(\tau)\rangle}{d\tau}=0\ . \tag{4.6}$$

Because $\langle\hat{\mathbf{v}}_\parallel(\tau)\rangle$ is proportional to N_1-N_2, where N_1 and N_2 are the number of neutrinos with mass m_1 and mass m_2, and because the total neutrino number N_1+N_2 is conserved, N_1 and N_2 are individually conserved. The conservation of individual mass-eigenstate numbers can be shown to hold generally for a pure neutrino gas with only neutral current interactions [13]. Since a time-averaging procedure violates N_1-N_2, it cannot arise in a pure neutrino gas but must be induced by other interactions such as the weak charged-current interaction. Background charged leptons can create and destroy neutrinos and lead to varying propagation times.

Equation (4.6) implies that $\langle\hat{\mathbf{v}}\rangle$ moves in a plane perpendicular to $\hat{\mathcal{B}}_0$. If $\langle\hat{\mathbf{v}}\rangle$ achieves a constant asymptotic value then $\lim_{\tau\to\infty}\langle\hat{\mathbf{v}}(\tau)\rangle$ is given by the projection of $\langle\hat{\mathbf{v}}(0)\rangle$ onto $\hat{\mathcal{B}}_0/\kappa$:

$$\lim_{\tau\to\infty}\langle\hat{\mathbf{v}}(\tau)\rangle=\cos(2\theta)(\cos(2\theta),-\sin(2\theta),0)\ , \tag{4.7}$$

so that

$$\lim_{\tau\to\infty}\langle\beta\rangle=\cos^2(2\theta)\ ,$$

which is the same result as for vacuum oscillations.

E. Numerical results for averaging over an energy distribution

This subsection presents numerical results for the case of a flat energy distribution. Such a distribution corresponds to a flat distribution in $1/\kappa$ and leads to different $\hat{\mathcal{B}}_0$ for different neutrinos. Suppose the neutrino interactions are neglected. Then, neutrinos with different energies have different oscillation times, λ_m, as can be seen from Eq. (3.11). Even when the neutrino wave functions begin in phase at $\tau=0$, one expects the phases to eventually distribute themselves randomly and for incoherence to be achieved. Hence, $\langle\beta\rangle$ and $\langle\beta_{e\mu}\rangle$ should have smooth limits and satisfy Eqs. (3.34) and (4.7):

$$\lim_{\tau\to\infty}[\langle\beta\rangle,\langle\mathrm{Re}(\beta_{e\mu})\rangle,\langle\mathrm{Im}(\beta_{e\mu})\rangle] = \cos(2\theta)(\cos(2\theta),-\sin(2\theta),0) .$$

For $\kappa_0>1$, this is the case. Figure 7 displays the results when $\sin^2(2\theta)=0.25$ and

$$\kappa_0=\Delta/2\sqrt{2}G_F E_0\rho_\nu=5.0 ,$$

where E_0 is the average energy. We used 101 neutrinos

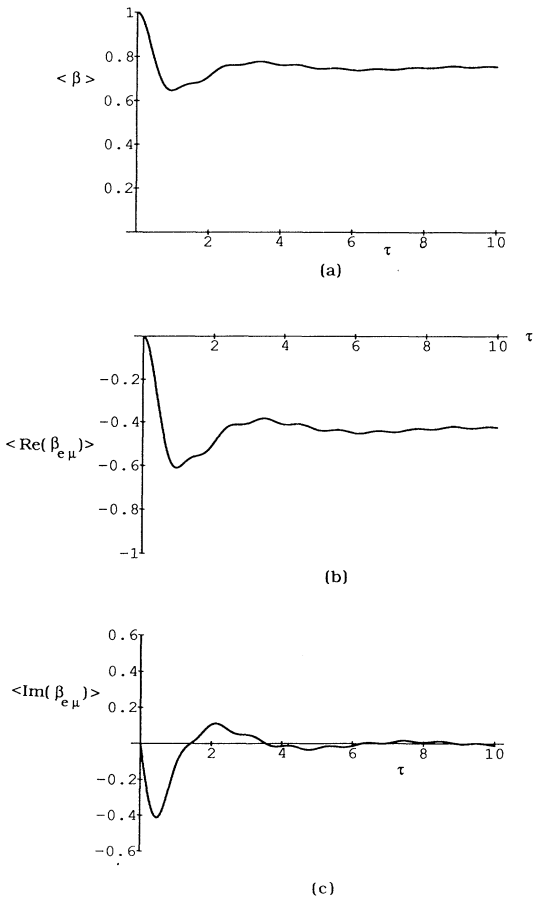

FIG. 7. The neutrino backgrounds for a low-density gas with an energy-averaging procedure as a function of time. The results are for $\kappa_0=5.0$, $\sin^2(2\theta)=0.25$, and a flat energy distribution with energies varying from $0.4E_0$ to $1.6E_0$.

with energies varying uniformly between $0.4E_0$ and $1.6E_0$. The asymptotic values are

$$\langle\beta\rangle\approx 0.75, \quad \langle\mathrm{Re}(\beta_{e\mu})\rangle\approx -0.43 ,$$

and

$$\langle\mathrm{Im}(\beta_{e\mu})\rangle\approx 0.00$$

in agreement with the predictions in Eq. (4.7) of 0.750, −0.433, and 0. In addition,

$$\langle\mathrm{Re}(\beta_{e\mu})\rangle/\langle\beta\rangle\approx -0.57$$

agrees with the theoretical result of $-\tan(2\theta)\approx -0.58$. We checked that results were not sensitive to N_ν when N_ν is large.

When we reduce κ_0 to 0.5, an unexpected phenomenon occurs. There is self-maintained coherence. Independent of N_ν and the total integration time, incoherence is not achieved. Figures 8(a), 8(b), and 8(c) display the neutrino backgrounds during the first few oscillation times. The oscillatory behavior continues indefinitely. We have observed it to persist beyond 250 oscillation times, i.e., for $\tau>5000$. Figures 8(d) and 8(e) show the behavior of θ_m and α_m. The former oscillates while $2\alpha_m$ continuously cycles around the unit circle. Neutrino-neutrino interactions cause neutrinos to bunch together in flavor space. Even though neutrino energies vary from $0.4E_0$ to $1.6E_0$, coherence is maintained and almost all the neutrinos oscillate in phase. The same phenomenon occurs for smaller values of κ_0.

By examining individual solutions, we believe we have an intuitive explanation of the above effect. Coherence is maintained if the vectors $\hat{\mathbf{v}}_\perp$ associated with different individual neutrinos rotate at approximately the same rate. Suppose a particular neutrino has an energy smaller than the average energy E_0, and, hence, a relatively large κ. Neglecting neutrino interactions, its $\hat{\mathbf{v}}_\perp(\tau)$ would rotate faster around $\hat{\mathcal{B}}_0$ than the $\hat{\mathbf{v}}_\perp(\tau)$ of a neutrino with energy E_0 because of the factor of κ in $\hat{\mathcal{B}}_0$ in Eq. (4.4). Taking into account the term $\langle\hat{\mathbf{v}}_\perp(\tau)\rangle\times\hat{\mathbf{v}}_\perp(\tau)$ in the equation for $d\hat{\mathbf{v}}_\parallel(\tau)/d\tau$ in Eq. (4.4), one sees $\hat{\mathbf{v}}_\parallel$ is reduced compared to a neutrino with an average energy. The situation is similar to back-time averaging. The smaller value of $\hat{\mathbf{v}}_\parallel$ causes $\hat{\mathbf{v}}_\perp(\tau)$ to rotate more slowing than a neutrino with energy E_0 due to the second term in Eq. (4.5). Hence the first two terms in Eq. (4.5) can cancel each other. Apparently, they maintain the $\hat{\mathbf{v}}_\perp(\tau)$ of different neutrinos rotating at the same rate on average. The last term in Eq. (4.5), $\langle\hat{\mathbf{v}}_\parallel\rangle\times\hat{\mathbf{v}}_\perp(\tau)$, does not make any of the $\hat{\mathbf{v}}_\perp(\tau)$ rotate faster or slower. In examining the orbit of $\hat{\mathbf{v}}(\tau)$ for the neutrino with energy $0.4E_0$ we observed that $\hat{\mathbf{v}}_\parallel(\tau)$ is reduced compared to neutrinos with energy E_0. The opposite was true for the neutrino with energy $1.6E_0$. When E is larger than E_0, the $\hat{\mathbf{v}}_\perp(\tau)\times\hat{\mathcal{B}}_0$ term in Eq. (4.5) affects a slower rotation for $\hat{\mathbf{v}}_\parallel$. However, $\hat{\mathbf{v}}$ spirals forward and $\hat{\mathbf{v}}_\parallel$ increases and this creates a faster rotation due to the $\langle\hat{\mathbf{v}}_\perp(\tau)\rangle\times\hat{\mathbf{v}}_\parallel(\tau)$ term. In other words, we believe the first two terms in Eq. (4.5) compensate for each other on average and this cancellation produces a lack of decoherence. This can only occur for κ_0 sufficiently small. When $\kappa_0>1$

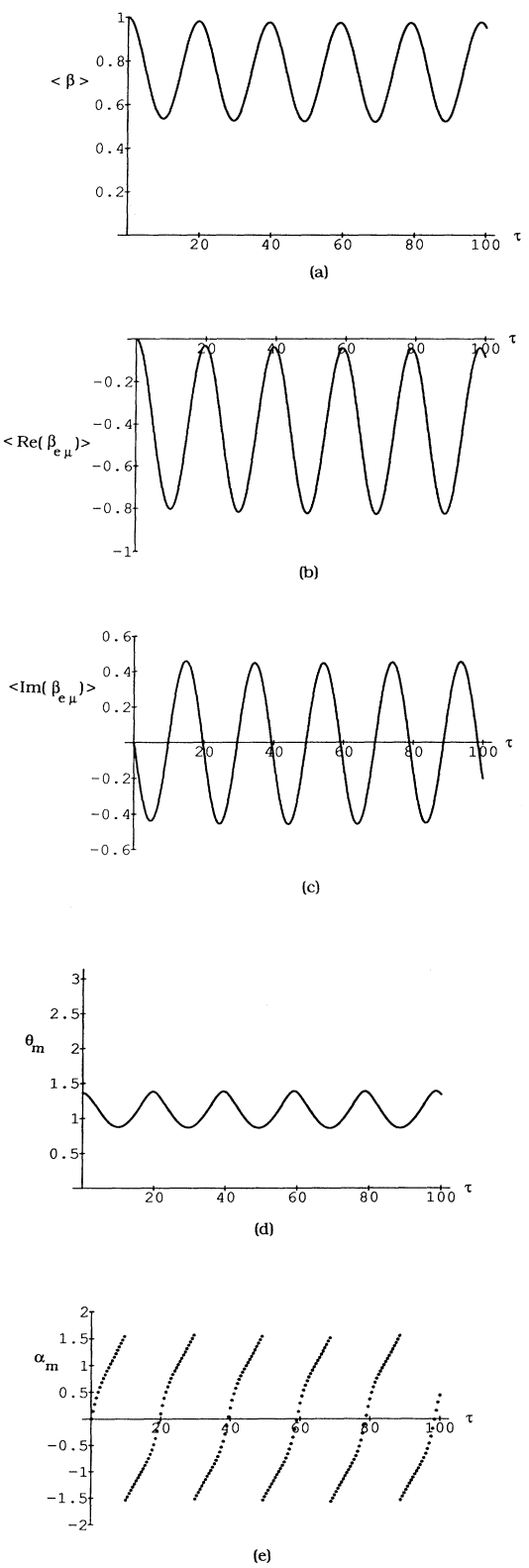

FIG. 8. The neutrino backgrounds and matter-induced angles for a high-density gas with an energy-averaging procedure. Only the first five or so oscillation times are shown. The behavior continues indefinitely. The parameters are the same as in Fig. 7 except $\kappa_0=0.5$.

the second term cannot completely cancel the first term in Eq. (4.5).

V. CONCLUSION

We have obtained a formalism for analyzing neutrino oscillations for a dense self-interacting neutrino gas. Three key ingredients were involved. The first was obtaining the correct and self-consistent equations. Although these equations determine the behavior of neutrino oscillations they involve an averaging procedure. The second key realization was that the physics depends on certain statistical distributions characteristic of and specific to the gas. An analysis cannot be commenced until neutrino energy distributions, density fluctuations, initial flavor states, etc. are specified. As a result, general conclusions cannot be drawn; a separate analysis must be performed for each type of gas. The third key step was the implementation of the self-consistency condition described in general in Sec. II and illustrated with examples in Sec. IV. The background neutrino currents and densities are determined from this condition. Because the concept of a neutrino gas is general, there should be many applications of our formalism.

The dense neutrino gas is a highly nonlinear system. In the examples treated in Sec. IV, striking phenomena were observed. Perhaps the most interesting is the self-induced MSW effect in which a gas of electron neutrinos changes into mostly muon neutrinos by resonant conversion. Unlike the usual MSW effect for which background electrons create the resonance, it is the neutrinos themselves which cause it. Another phenomenon observed for one type of gas was parametric resonance. A relatively dilute gas of electron neutrinos slowly converted itself into a gas of muon neutrinos. The interaction effects of neutrinos were greatly enhanced over long periods of time due to the nonlinear nature of the problem. Finally, we observed self-maintained coherence for a particular gas in which decoherence was expected. The oscillations of a large fraction of the neutrinos remained in phase and decoherence was not achieved on any time scale.

There remains much research to do. In Sec. IV, certain idealized averaging procedures were considered. They were used to exhibit the possible behaviors of dense neutrino gases. Other types of statistical distributions are of physical interest, should be incorporated, and should be analyzed. Furthermore, we have used only one at a time. Real systems involve many distributions. Future investigations should focus on other averaging procedures, choosing different initial neutrino conditions and incorporating several statistical distributions simultaneously. It is useful to know what other kinds of phenomena arise for dense neutrino gases.

For one type of gas in one region of parameter space, we were unable to find an algorithm to implement the self-consistency condition. We do not know whether the lack of convergence is due to a breakdown of the iterative procedure or due to the nature of the gas itself. For example, if the system were chaotic, one would not expect convergence. It would be interesting to develop other methods for finding neutrino background densities and to

investigate whether certain gases possess chaotic behavior.

Because the physics depends on the detailed nature of the gas, it is probably best to proceed by applying the formalism to known systems in nature. Possible applications include effects in the early Universe and in supernova explosions. We are currently investigating the behavior of neutrino oscillations in the early stages of the universe [18].

Note added. After this manuscript was accepted for publication, a paper appeared [19] which also incorporates the off-diagonal terms correctly.

ACKNOWLEDGMENTS

The author is grateful to Jim Pantaleone for pointing out to him the existence of the unsolved problem of a dense neutrino gas and for many fruitful discussions. He thanks Alan Kostelecký, Don Lichtenberg, and Jim Pantaleone for suggestions concerning the manuscript. He is grateful to these three and Archie Hendry for hospitality at Indiana University and for conversations on neutrino physics.

APPENDIX: TAYLOR-SERIES EXPANSIONS

For small times, accurate analytical results can be obtained via Taylor series. For the time-averaging procedure we expand using

$$\hat{\mathbf{v}}(\tau)=\sum_{j=0}^{\infty}\mathbf{a}_j\tau^j,\quad \langle\hat{\mathbf{v}}(\tau)\rangle=\sum_{j=0}^{\infty}c_j\mathbf{a}_j\tau^j\ , \tag{A1}$$

where the definition of the averaging moment coefficients c_j is

$$\tau^j c_j\equiv\frac{1}{\tau(f_m+f_p)}\int_{\tau(1-f_m)}^{\tau(1+f_p)}d\sigma\,\sigma^j \tag{A2}$$

or

$$c_0=1,\quad c_j=\frac{1}{(f_m+f_p)}[(1+f_p)^{j+1}-(1+f_m)^{j+1}]\ . \tag{A3}$$

The coefficients $\mathbf{a}_n$ are determined from Eq. (3.25). One finds

$$\mathbf{a}_n=\frac{1}{2n}\left[\sum_{j=0}^{n-1}c_j\mathbf{a}_j\times\mathbf{a}_{n-j-1}+\mathbf{a}_{n-1}\times\hat{\mathcal{B}}_0\right]\ . \tag{A4}$$

Equation (A4) permits an inductive determination of the $\mathbf{a}_n$. When

$$\hat{\mathbf{v}}(0)=\langle\hat{\mathbf{v}}(0)\rangle=(1,0,0)\ ,$$

$\mathbf{a}_0=(1,0,0)$ and the first few terms in Eq. (A1) are

$$\begin{aligned}
&\beta=1-\tfrac{1}{8}(\kappa s_{2\theta}\tau)^2+O(\tau^3)\ ,\\
&\beta_{e\mu}=-\frac{i\kappa s_{2\theta}\tau}{2}-\frac{s_{2\theta}c_{2\theta}}{8}(\kappa\tau)^2+\frac{\kappa s_{2\theta}}{8}(1-c_1)\tau^2+O(\tau^3)\ ,\\
&\langle\beta\rangle=1-\frac{c_2}{8}(\kappa s_{2\theta}\tau)^2+O(\tau^3)\ ,\\
&\langle\beta_{e\mu}\rangle=-\frac{ic_1\kappa s_{2\theta}\tau}{2}-\frac{c_2 s_{2\theta}c_{2\theta}}{8}(\kappa\tau)^2\\
&\qquad+\frac{c_2\kappa s_{2\theta}}{8}(1-c_1)\tau^2+O(\tau^3)\ ,
\end{aligned} \tag{A5}$$

where $s_{2\theta}\equiv\sin(2\theta)$, $c_{2\theta}\equiv\cos(2\theta)$, and

$$\hat{\mathbf{v}}=(\beta,\mathrm{Re}(\beta_{e\mu}),\mathrm{Im}(\beta_{e\mu}))\ .$$

For energy averaging, let $\hat{\mathbf{v}}^{(i)}(\tau)$ and $E^{(i)}$ be, respectively, the flavor vector and the energy for the ith neutrino. Expand using

$$\hat{\mathbf{v}}^{(i)}(\tau)=\sum_{j=0}^{\infty}\mathbf{a}_j^{(i)}\tau^j,\quad \langle\hat{\mathbf{v}}(\tau)\rangle=\sum_{j=0}^{\infty}\langle\mathbf{a}_j\rangle\tau^j\ . \tag{A6}$$

Then

$$\mathbf{a}_n^{(i)}=\frac{1}{2n}\left[\sum_{j=0}^{n-1}\langle\mathbf{a}_j\rangle\times\mathbf{a}_{n-j-1}^{(i)}+\mathbf{a}_{n-1}^{(i)}\times\hat{\mathcal{B}}_0^{(i)}\right]\ ,$$

$$\langle\mathbf{a}_j\rangle=\frac{1}{N_\nu}\sum_{i=1}^{N_\nu}\mathbf{a}_n^{(i)}\ , \tag{A7}$$

allows one to determine the Taylor-series coefficients inductively. In Eq. (A7)

$$\hat{\mathcal{B}}_0^{(i)}\equiv\kappa^{(i)}(\cos(2\theta),-\sin(2\theta),0)\ ,$$

where

$$\kappa^{(i)}\equiv\Delta/2\sqrt{2}G_F E^{(i)}\rho_\nu\ .$$

[1] E. W. Kolb and M. S. Turner, *The Early Universe* (Addison Wesley, Redwood City, CA, 1990).
[2] L. Wolfenstein, Phys. Rev. D **17**, 2369 (1978); **20**, 2634 (1979).
[3] S. P. Mikheyev and A. Yu. Smirnov, Yad. Fiz. **42**, 1441 (1985) [Sov. J. Nucl. Phys. **42**, 913 (1985)].
[4] J. Bahcall, *Neutrino Astrophysics* (Cambridge University Press, Cambridge, England, 1989).
[5] See, for example, R. N. Mohapatra and P. B. Pal, *Massive Neutrinos in Physics and Astrophysics* (World Scientific, Singapore, 1991).
[6] See, for example, R. N. Mohapatra, *Unification and Supersymmetry* (Springer-Verlag, New York, 1992).
[7] A. D. Dolgov, Yad. Fiz. **33**, 1309 (1981) [Sov. J. Nucl. Phys. **33**, 700 (1981)].
[8] G. M. Fuller, R. W. Mayle, J. R. Wilson, and D. N. Schramm, Astrophys. J. **322**, 795 (1987).
[9] L. Stodolsky, Phys. Rev. D **36**, 2273 (1987).
[10] D. Notzold and B. Raffelt, Nucl. Phys. **B307**, 924 (1988).
[11] R. Barbieri and A. Dolgov, Phys. Lett. B **237**, 440 (1990).
[12] M. J. Thomson and B. J. McKellar, Phys. Lett. B **259**, 113 (1991).

[13] J. Pantaleone, Phys. Rev. D **46**, 510 (1992).
[14] J. Pantaleone, Phys. Lett. B **287**, 128 (1992).
[15] T. K. Kuo and J. Pantaleone, Rev. Mod. Phys. **61**, 937 (1989).
[16] V. K. Ermilova, V. A. Tsarev, and V. A. Chechin, Kratk. Soobshch. Fiz. **5**, 26 (1986).
[17] E. Akhmedov, Yad. Fiz. **47**, 475 (1988) [Sov. J. Nucl. Phys. **47**, 301 (1988)].
[18] V. A. Kostelecký, J. Pantaleone, and S. Samuel, "Neutrino Oscillations in the Early Universe," Indiana University Report No. IUHET 251, 1993 (unpublished).
[19] G. Sigl and G. Raffelt, "General Kinetic Description of Relativistic Mixed Neutrinos," Max-Planck-Institut Report No. MPI-Ph/92-112 (unpublished).